# CRACK DETECTION USING EDDYTHERM

G. Zenzinger, J. Bamberg, M. Dumm, P. Nutz

MTU Aero Engines, D-80995 Munich, Germany

**Abstract -** The EddyTherm thermographic crack detection method uses brief pulsed eddy currents to heat metallic components under inspection. Cracks, if present, will disturb the current flow and so generate changes in the temperature profile in the crack area. These temperature changes are visualized using a thermographic camera.
The advantages afforded by the method are its very brief inspection times, its ability to inspect complex geometries, its excellent flaw detection sensitivity and its ability to detect hidden, subsurface cracks. Simulation of inductive heating using FEM methods permits coils to be adjusted and inspection parameters optimized.
The use of a robot to manipulate parts under inspection, a high-frequency pulse generator for inductive heating and enhanced algorithms enabled a demonstrator to be set up for the fully automated crack inspection of engine compressor blades.

## INTRODUCTION

In many industries, crack inspection is a valuable nondestructive test method. This holds true also when it is used on engine components, which often exhibit complex geometries, are exposed to high thermal and mechanical loads and are expected to satisfy stringent safety requirements. Accordingly, there is a growing need for powerful crack detection methods.

In this context, thermography has increasingly gained in significance these past several years. Focused development of thermography in combination with eddy current inspection has resulted in the EddyTherm inspection method [1, 2].

Historically, inductive heating has been employed chiefly for materials processing, such as hardening or induction welding. In the process, high-frequency generators generate, through induction coils, continous alternating magnetic fields that cause the current to flow and the part under inspection to heat up rapidly. The EddyTherm method uses brief 50-200 ms high-frequency pulses to heat the part to a moderate, defined overall temperature. In the process, cracks disturb the flow of the induced currents and affect the temperature distribution on the part surface so that cracks can be visualized using a suitable thermographic camera [3]. Fig. 1 is a schematic representation showing the changed current flow through the crack and the resultant temperature rise at the crack tips and the associated colder regions at the crack flanks.

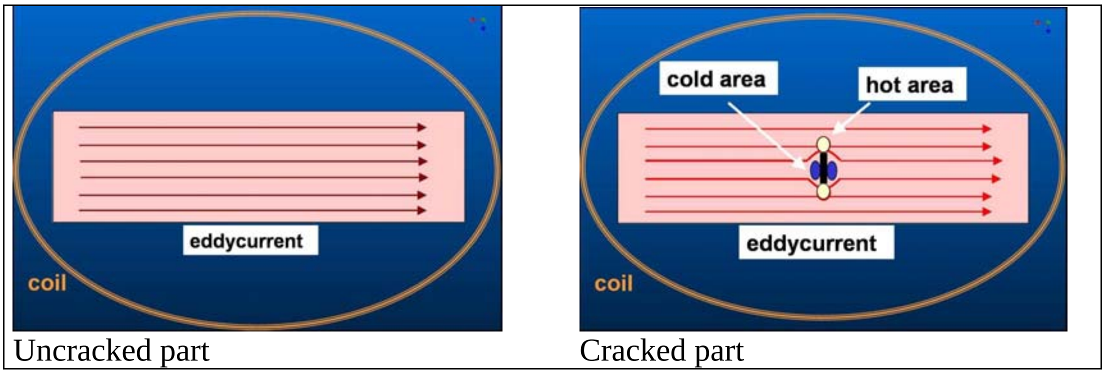


**Fig. 1.** EddyTherm principle

An important aspect of all inductive methods is the so-called skin effect, where the induced current's depth of penetration (skin depth) into the material varies with the frequency of the magnetic field and the relative permeability of the material under inspection:

skin depth $$\delta = \sqrt{\frac{2\rho}{\omega\mu}}$$

angular frequency $\omega = 2\pi f$

permeabiliy $\mu = \mu_0 \mu_r$

resistivity $\rho$

For detecting small cracks, a moderate skin depth provides an advantage since a preferably large portion of the induced current flows around the crack, maximizing the changes in current density and hence the temperature differences. Playing an important role also is the relative permeability ($\mu_r$) of the material. With paramagnetic materials, it is practically unity, while with ferromagnetic materials, it may be as high as 50-80,000. The effect of the excitation frequency for ferromagnetic and paramagnetic materials is shown in Fig. 2.

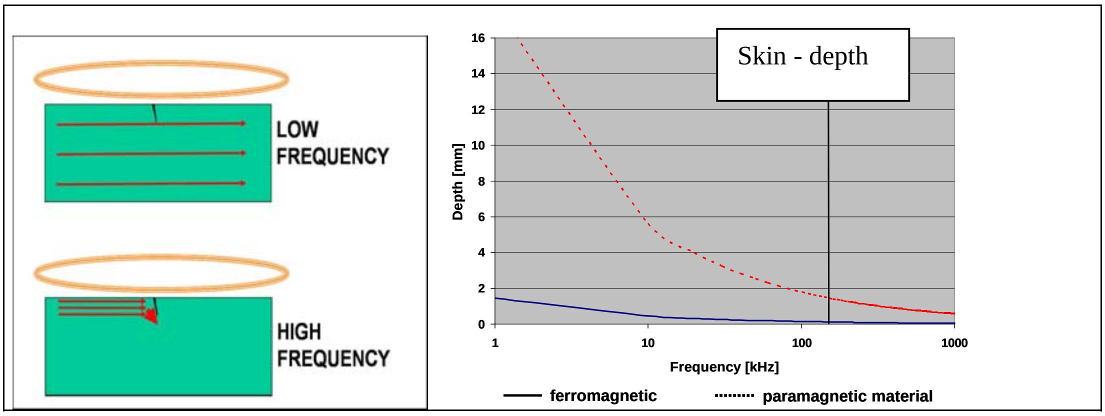


**Fig. 2.** Effect of excitation frequency and magnetic properties

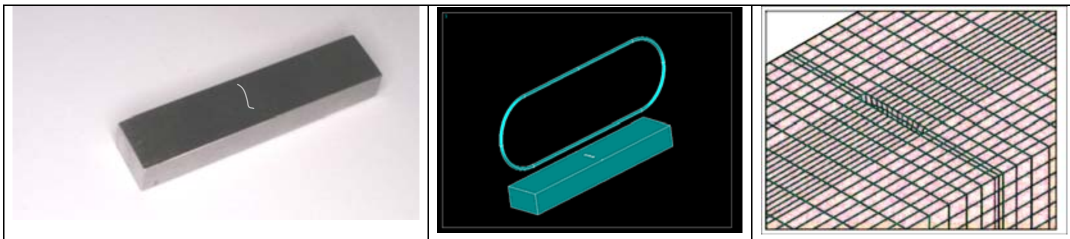

Cracked metallic specimen
L x W x H = 50 x 10 x 6 mm

FEM grid

Detail view with crack

**Fig. 3.** Specimen for FEM simulation

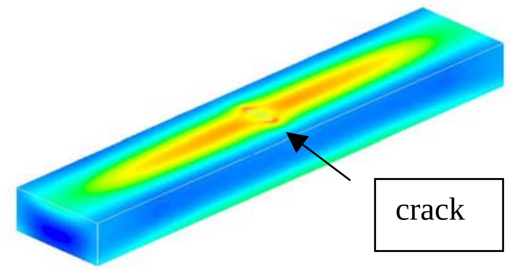


**Fig. 4.** Computed temperature profile in a cracked metallic specimen (pulse length 200 ms)

## FEM SIMULATION: CRACKED PLAIN SPECIMEN

To optimize the test specimen-coil arrangement, FEM simulation of the inductive heating process will be helpful, as here demonstrated using a cracked cuboid.

The changed temperature profile in the crack area becomes clearly apparent (Fig. 4). At the crack tips, the anticipated temperature rise relative to the colder regions at the test flanks is evident.

## SPECIMEN MATERIAL

For investigations under the process development effort, use was made of the following specimens exhibiting artificial or real cracks:

**Table 1.** Specimen material

| Specimen No. | Description | Crack size **L**ength x **W**idth x **D**epth | Type |
|---|---|---|---|
| 1 | 4-point bend specimen | L= 3 mm | Real crack |
| 2 | Turbine blade | L= 2 mm | Real crack |
| 3 | Cuboid | L=0.4; W=0.06; D=0.12 mm | Eroded notch |
| 4 | Cuboid | Crack 1: L=0.9; W=0.1; D=0.4 mm | Eroded notch |
| | | Crack 2: L=0.4; W=0.08; D=0.2 mm | Eroded notch |

In the four-point bending specimen, the crack was caused by mechanical fatigue load. In the turbine blade, a crack was caused by using inappropriate parameters when grinding the blade root.

## Test of specimen No. 1 – four-point bend specimen

The specimen under test is arranged within an induction coil which through a transformer connects to a high-frequency generator. The camera has an unobstructed view of the component surface between the coil windings (Fig. 5). The HF generator and the camera are controlled from a PC. The HF generator was specifically developed for the EddyTherm method. It is a variable 50-200 ms pulse length generator with an ac power of 2 kW. As a special feature, the system can operate with uncooled coils. Evaluation of the thermography image sequences is made using suitable image processing software. The image data is provided in the software in near-real time, so that a test merely takes a few seconds.

The results here presented were all obtained from test specimens or components with metallic, not blackened surfaces.

In the EddyTherm image (Fig. 6), the crack (length 3 mm) is clearly apparent. As in the simulation, the presence of warmer regions at the crack tips and colder regions at the crack flanks is demonstrated.

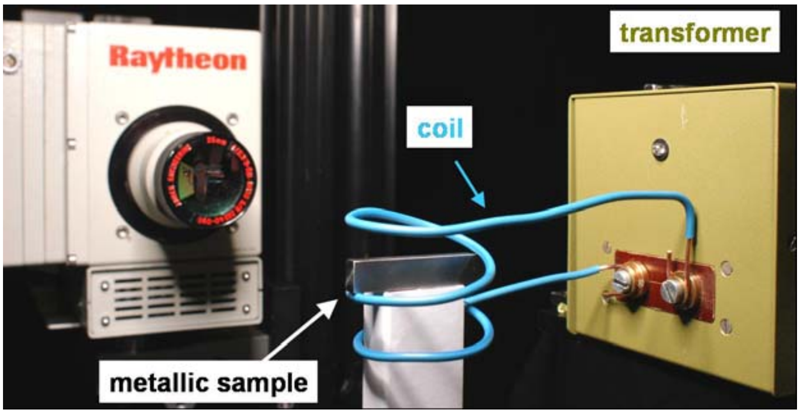


**Fig. 5.** Test setup including IR camera, specimen, transformer and coil

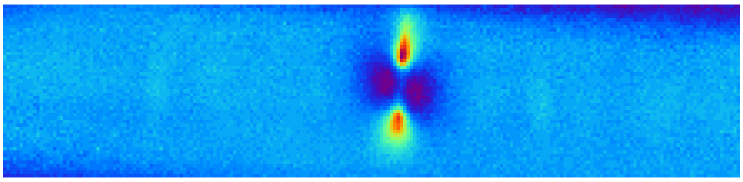

**Fig. 6.** EddyTherm image of cracked 4-point bend specimen (specimen No. 1)

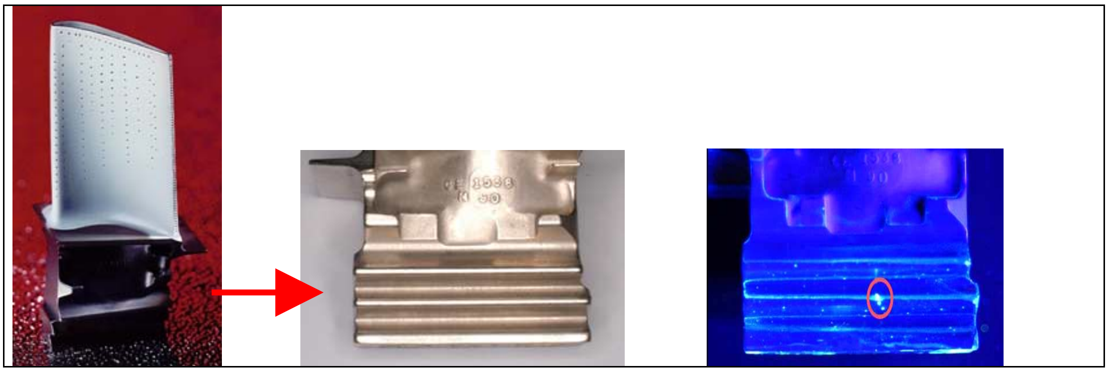

**Fig. 7.** CF6 turbine blade (specimen No. 2) with close-up view of blade root and FPI crack indication

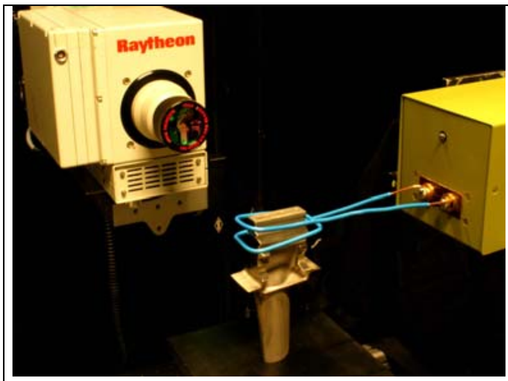


**Fig. 8.** Test setup for CF6 turbine blade root

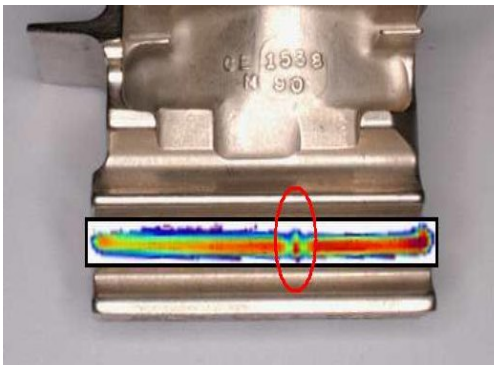

**Fig. 9.** Inspection result: crack in turbine blade (specimen No. 2)

**<u>Typical inspection on turbine blade</u>**

During the grinding process, cracks may arise in the flanks of turbine blade roots (Fig. 7). Such cracks must be detected without fail. The current practice is to use fluorescent penetrant inspection (FPI) for the purpose.

Fig. 8 illustrates the EddyTherm test setup. The coil is positioned around the blade root in a manner that does not obstruct the IR camera's free view of the root flanks under inspection.

To elucidate relationships, the EddyTherm image was projected onto a photograph of the blade root. As previously on the FPI image, the crack is clearly apparent (Fig. 9).

## DEFECT DETECTION LIMITS

In crack inspection, the smallest size down to which defects can still be detected plays an important part. In an attempt to optimize the inspection process, therefore, specimens possessing artificial (eroded) and real (mechanical fatigue load-induced) cracks were manufactured. The size of the smallest eroded crack was 0.4 mm long and 0.2 mm deep (specimen No. 3). Owing to the heavily changed emission coefficient in the eroded areas-

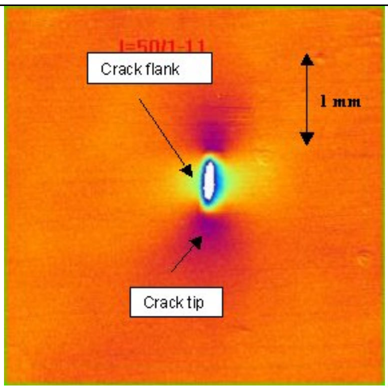


**Fig. 10.** EddyTherm image showing eroded crack 0.4 mm. long and 0.2 mm. deep (specimen No. 3).

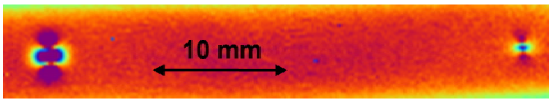


**Fig 11.** Titanium specimen with artificial, eroded cracks (specimen No. 4)

from the radiation aspect, small fissures act like small black body radiators-evaluation of the thermal images was necessarily limited to the crack flanks and tips. Fig. 10 shows the image resulting from the smallest crack. Apart from the emission signal of the discontinuity, it is clearly apparent that at the ends of the fissure the specimen material is hotter than elsewhere. With the EddyTherm principle (typical current density rise at the crack tips is present), therefore, a crack of this size can still be detected.

The exposure (Fig.10) was made using a geometrically high-resolution lens. The frame size is about 3.5 mm x 3.5 mm At this resolution, cost-effective inspection of larger areas is prevented.

Another specimen was therefore inspected at a frame size of 60 mm x 60 mm. In this titanium specimen, two artificial cracks were eroded, one 0.9 mm long and 0.4 mm deep and the other 0.4 mm long and 0.2 mm deep (specimen No. 4). At these exposure conditions, too, the typical EddyTherm signals of the cracks were detected (Fig. 11).

In the EddyTherm image, the crack indications are appreciably blown up over actual crack dimensions, because the signals (hot spot at the crack tip and cold spot at the crack flank) were outside the actual crack. This effect is again boosted by the transverse heat conduction in the metallic material.

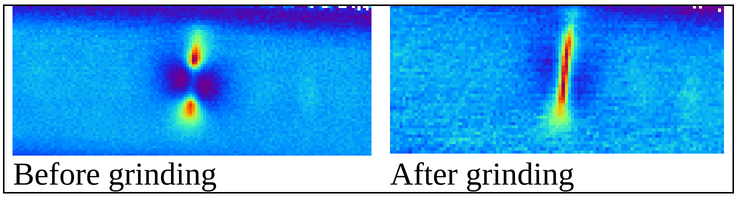


**Fig. 12:** Crack in 4-point bend specimen (specimen No. 1)

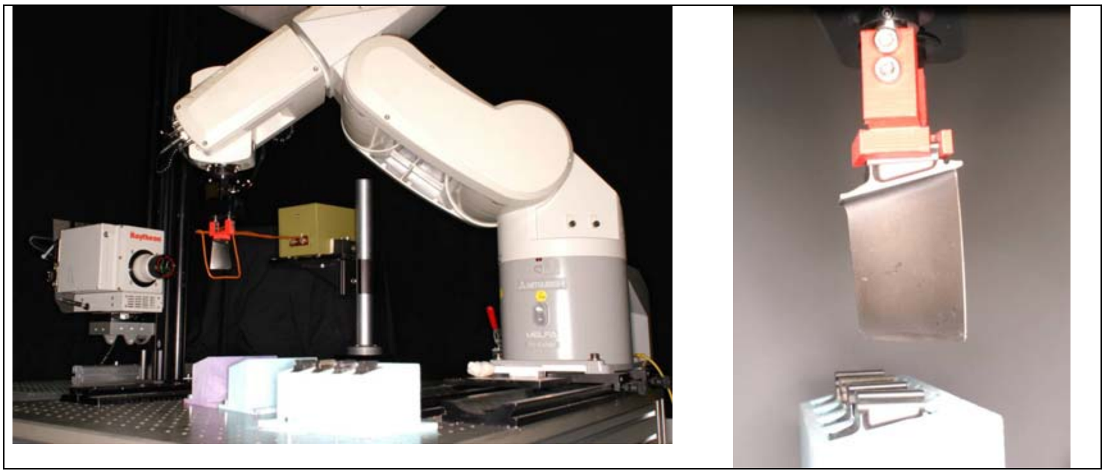

**Fig. 13.** Automated inspection of compressor blades, with a close-up view of the blade holder on the robot arm

## HIDDEN CRACKS

At this time, it is often very difficult if not impossible to safely detect cracks that are smeared by processing operations or concealed under coatings. The HF systems used at MTU operate with excitation frequencies of 100 to approximately 550 kHz. This enables relatively large skin depths of about 1 mm to be achieved. These systems, therefore, should readily witness masked cracks under conductive material [4].

The four-point bend specimen (specimen No. 1) with its real crack was therefore ground in a manner that smeared the crack with grinding debris. This made the crack undetectable by FPI. Fig. 12 (left) again shows the known EddyTherm signal of the open crack The right-hand image shows, after grinding, the full length of the crack.. The current here flows through the smeared material across the crack and so causes uniform heating over the length of crack. The crack accordingly remains detectable by EddyTherm.

## AUTOMATION

One of the essential advantages the EddyTherm method affords over FPI is that it lends itself to automation.  To prove its automation potential, a demonstrator was built for inspecting compressor blades from an aero engine (Fig. 13). In this setup, the blades are taken by a robot from a magazine, positioned in front of the induction coil, heated to a defined temperature and then photographed by the thermographic camera. Evaluation of the thermal image sequences is automatic, through an image processing system. Uncracked components are then deposited apart from defective blades.

## SUMMARY AND PROSPECTS

These investigations witness the substantial application potential of the EddyTherm crack inspection method. Its defect detection limits are on the same order of magnitude (crack length x depth = 0.4 x 0.12 mm) as that of conventional techniques. The inspections were all conducted on unconditioned, partially even slightly contaminated components. This is to say that the EddyTherm technique does not require elaborate treatment or cleaning before inspection. This may prove a crucial cost aspect in testing during routine inspection or maintenance work. Another significant advantage afforded by the method is that it will detect also masked cracks, or cracks under coatings, and that it does so practically regardless of the surface texture. This marks an important advance in nondestructive testing work.

A typical application would be the overhaul of engine blades. During the inspection cycle, these are often stripped, crack-inspected and recoated. The costs involved could be substantially reduced through the use of EddyTherm. And since the method has potential for automation in both the inspection proper and subsequent evaluation, EddyTherm may before very long prove a practical, fast and reliable inspection option in production use.

## REFERENCES


1. Sakagami T. and Kubo S. JSME International Journal, Series A, Vol. 44, 2001 pp. 528-534
2. Maldague X. Nondestructive Evaluation of Materials by Infrared Thermography, 1993, Springer-Verlag
3. Riegert G., Zweschper T., Dillenz A. and Busse G., Wirbelstromangeregte Lockin-Thermografie – Prinzip und Anwendungen, DGZfP Dach-Jahrestagung 2004 Salzburg
4. Bamberg J. and Zenzinger G., European Patent No. 1069430A1 (17 Jan. 2001)